Cooperative Instabilities of Counterpropagating Light Waves in Homogeneous Plasma

G. G. Luther[a] and C. J. McKinstrie

Laboratory for Laser Energetics, 250 East River Road, Rochester, New York 14623

(Received 30 September 1991)

Filamentation and Brillouin-enhanced four-wave-mixing instabilities caused by the cooperative interaction between two counterpropagating electromagnetic waves are shown to possess larger convective growth rates and smaller absolute instability thresholds than the conventional single-pump instabilities. These cooperative instabilities may be important in certain laser-plasma interaction experiments.

PACS numbers: 52.35.Mw, 42.65.Hw, 42.65.Vh

The interference pattern of a strong electromagnetic pump wave beating with one of its electromagnetic sidebands drives ion waves ponderomotively in a plasma. These stimulated ion modes act as gratings in the index of refraction, scattering the pump wave and diverting its energy to the sidebands. Properly phase matched, the feedback of the pump into the sidebands leads to stimulated Brillouin scattering (SBS) or filamentation [1,2], also known as the transverse modulational instability (TMI). Both of these instabilities require only one pump wave interacting with either one or two sidebands. In this Letter we examine instabilities caused by the cooperative interaction of two counterpropagating (CR) pump waves.

In laser-plasma interactions, CR pump waves arise when the incident pump laser is reflected from the critical density surface or is parametrically backscattered from the underdense plasma region. Burnthrough light, which penetrates the target after the plasma is formed, may also act as a source for the CR pump. The CR waves are applied externally when the laser-plasma interaction is used for phase conjugation (PC).

In previous studies, a CR wave was shown to increase backward SBS by seeding the Stokes sideband [3,4]. In contrast, cooperative instabilities can have larger growth rates than single-pump instabilities and need not have single-pump analogs. Both thermal [5] and ponderomotive [6] filamentation are absolutely unstable when driven by CR pumps in plasmas. Cooperative TMI's [6–9] and longitudinal cooperative Brillouin-enhanced four-wave mixing (FWM) instabilities [10,11] have been shown to exist in other nonlinear optical materials. Absolute PC instabilities have also been shown to exist both in plasmas [12] and in other materials [13]. In this Letter, the first unified treatment of filamentation, near-forward, and near-backward SBS of CR light waves is presented.

Let a pair of intense, CR light waves $\mathbf{F}$ and $\mathbf{B}$ irradiate opposite ends of a uniform plasma. Each wave has a Stokes ($\omega_0-\omega^*$, $\pm\mathbf{k}_0-\mathbf{k}$) and an anti-Stokes ($\omega_0+\omega$, $\pm\mathbf{k}_0+\mathbf{k}$) sideband. The pump-wave envelopes $\mathbf{F}_0$ and $\mathbf{B}_0$ are initially uniform in the transverse coordinate, and the sideband envelopes $\mathbf{F}_\pm$ and $\mathbf{B}_\pm$ introduce perturbations of the form $\exp[\pm i\mathbf{k}_\perp\cdot\mathbf{r}]$. By requiring all six waves to be linearly polarized in the same direction and $|\mathbf{k}_\perp|/|\mathbf{k}_0|\ll 1$, only the near-forward and near-backward scattering instabilities are treated.

The evolution of the fields is governed by the electromagnetic wave equation driven by the nonlinear plasma current. The perturbed number density of the plasma couples to the fields through this current and is governed by the ponderomotively driven sound-wave equation [14]. The equations for the sidebands resulting from linearization of this standard model become

$$L\mathbf{A}=N\mathbf{A}, \tag{1}$$

where $\mathbf{A}=(F_+,F_-^*,B_+,B_-^*)^T$. The propagation matrix L is diagonal, having entries

$$L_{jj}=-i^{2j}(iv\partial_x+\omega)-c^2k_\perp^2/2\omega_0,\quad j=1,2, \tag{2}$$

where $v=c^2k_0/\omega_0$; L_{33} and L_{44} are obtained from L_{11} and L_{22}, respectively, by the substitution $v\rightarrow -v$.

Terms in each entry of the coupling matrix N correspond to gratings produced by the beating of the fields. The response of the gratings is characterized by $\Gamma(\omega,k)=c_s^2k^2(\omega^2+2i\nu_{ia}\omega-c_s^2k^2)^{-1}$ [12], where ν_{ia} is the phenomenological ion-acoustic damping rate. The CR wave system drives two resonant short-wavelength gratings, $\Gamma_\parallel=\Gamma(\omega,\pm 2\mathbf{k}_0+\mathbf{k}_\perp)$, a resonant long-wavelength grating, $\Gamma_\perp=\Gamma(\omega,\mathbf{k}_\perp)$, and a static grating, $\Gamma=1$. The elements of N are

$$N_{11}=\alpha[\Gamma_\perp F_0^2+(\Gamma_\parallel-1)B_0^2], \tag{3}$$

$$N_{12}=\alpha\Gamma_\perp F_0^2, \tag{4}$$

$$N_{13}=\alpha(\Gamma_\perp+1)F_0B_0^*, \tag{5}$$

$$N_{14}=\alpha(\Gamma_\perp+\Gamma_\parallel)F_0B_0, \tag{6}$$

where $\alpha=-Zm_e\omega_c^2/8m_i\omega_0c_s^2$. The remainder of the terms are $N_{ij}=N_{ji}^*$, $N_{22}=N_{11}$, $N_{23}=N_{14}^*$, $N_{24}=N_{13}$, $N_{33}=N_{44}=N_{11}(F_0\leftrightarrow B_0)$, and $N_{34}=N_{12}(F_0\leftrightarrow B_0)$.

Single-pump backward SBS is mediated by a sound wave which couples each sideband to its respective CR pump. Terms in N proportional to $\Gamma_\parallel-1$ characterize this interaction. Backward SBS grows as $\gamma L/v=(\alpha F_0^2L/v)^{1/2}[k_0L(c_s/c)(c/v)]^{1/2}$ [1,2]. Single-pump near-forward SBS and filamentation are mediated by the $\Gamma_\perp$ grating, which couples a pump wave to both its Stokes and anti-Stokes sidebands. The peak growth rate for single-wave filamentation is αF_0^2 (αB_0^2) for the forward (backward) pump, where the grating is driven nonresonantly at $\omega=0$.

Cooperative instabilities are driven by the action of

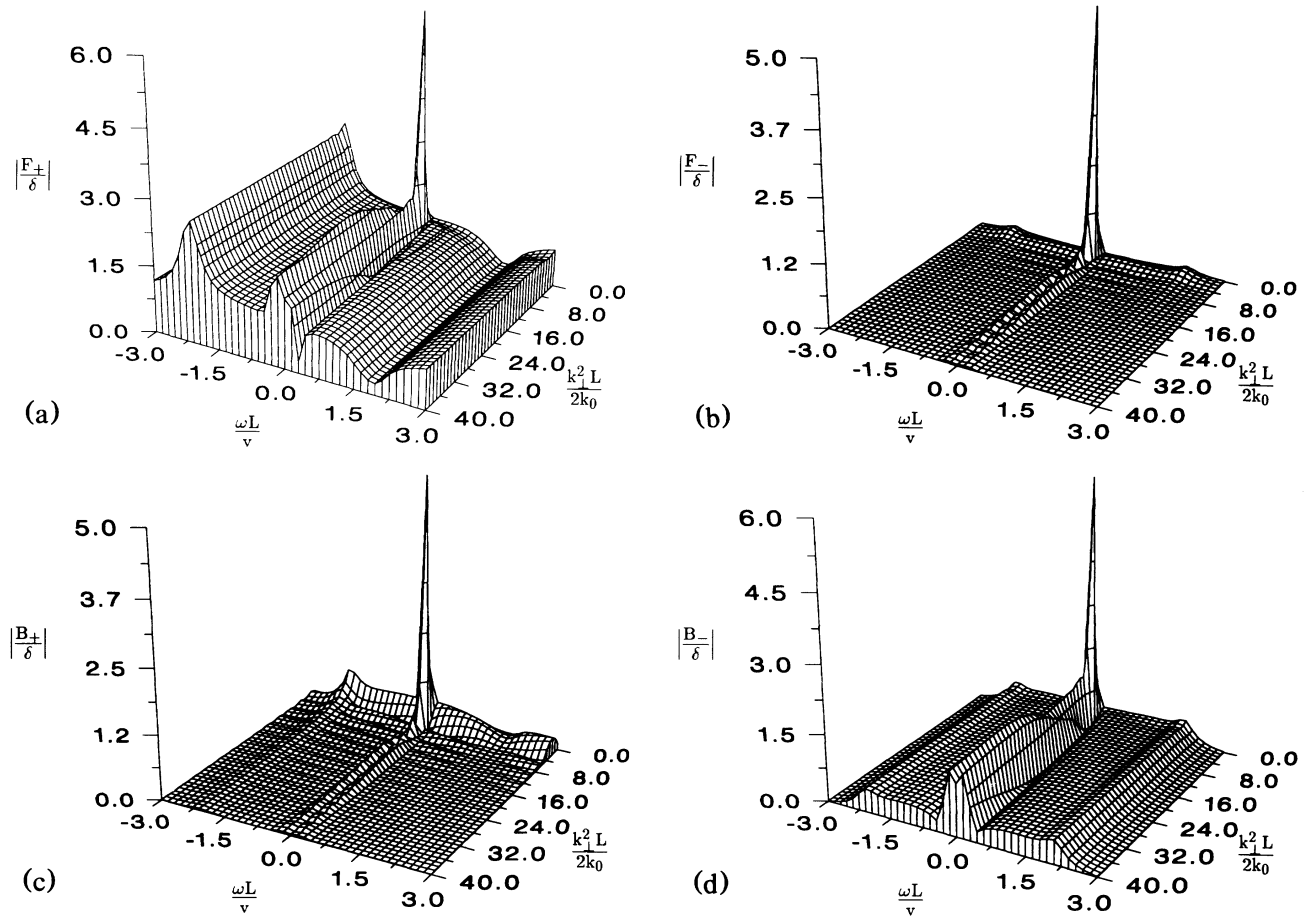

FIG. 1. Convective gain spectrum of (a) the seeded sideband, and its (b) forward FWM, (c) Bragg scattering, and (d) PC counterparts.

both pump waves. The two PC interactions couple Stokes shifted sidebands to their CR anti-Stokes shifted sidebands through the $\Gamma_\parallel$, $\Gamma_\perp$, or the static grating. Two Stokes or two anti-Stokes shifted sidebands couple through either the $\Gamma_\perp$ or static grating due to Bragg scattering by FWM. The cooperative filamentation of CR waves is the four-sideband analog of single-pump filamentation. The simultaneous action of PC, Bragg scattering, and single-pump filamentation drives the $\Gamma_\perp$ grating nonresonantly to produce a four-sideband instability.

These single-pump and cooperative instabilities can be identified in the linear convective gain spectrum of the four sidebands. In Fig. 1, the single-pass convective gain of each sideband is plotted as a function of $k_\perp^2 L/2k_0$ and $\mathrm{Re}(\omega L/v)$, the real part of the perturbation frequency, for $B_0^2 = F_0^2$, $c_s/c = 0.001$, $k_0 L = 1000$, and $\nu_{ia}/\Omega_{ia} = 0.2$, where Ω_{ia} is the ion-acoustic frequency. The pump power is $\alpha F_0^2 L/v = 0.43$ which is 0.95 of the minimal absolute threshold intensity for cooperative filamentation [6–8]. These spectra were calculated by numerically integrating the coupled-mode equations (1)–(6) with $B_\pm(L) = 0$, $F_-(0) = 0$, and $F_+(0) = \delta$, where $F_+(0)$ seeds the interaction and $\delta \ll 1$. Peaks in the gain occur when the sidebands are oriented and spectrally tuned such that their linear and nonlinear phase shifts are optimally matched inside the medium, where the beat frequency and wave number correspond to the frequency-degenerate gratings, the resonant $\Gamma_\perp$ gratings, or the resonant $\Gamma_\parallel$ gratings. Peaks in the convective gain spectrum which occur at finite $k_\perp^2$ indicate the presence of transverse structure, where the scattering angle $\theta^2 \approx 2(k_\perp^2 L/2k_0)/k_0 L$.

At large $k_\perp$, pure PC between F_+ and B_- due to both resonant and nonresonant gratings is recovered, as seen in Fig. 1(d). Near $k_\perp^2 = 0$ for $\mathrm{Re}(\omega L/v)$ near neither zero nor one of the ion-acoustic resonances, single-pump filamentation due to F_+ and F_- is recovered [see Fig. 1(b)]. For $k_\perp^2 L/2k_0 \sim \mathrm{Re}(\omega L/v) \gg 1$ in Fig. 1(c), nonresonant Bragg scattering due to F_+ and B_+ is recovered [9].

For smaller values of $k_\perp^2$, where $\mathrm{Re}(\omega L/v)$ is near zero or one of the ion-acoustic resonances, the one- and two-sideband instabilities overlap causing hybrid instabilities

[9]. The largest convective gain in Fig. 1, located near $\mathrm{Re}(\omega L/v)=0$ and $k_\perp^2 L/2k_0=3.1$ for each sideband, is due to cooperative filamentation [9]. Backward SBS is detuned as ω deviates from the ion-acoustic frequency, so $\Gamma_\parallel - 1 \to 0$ when $\omega \to 0$ at fixed $k_\perp$. Backward SBS shares the $\Gamma_\parallel$ resonance with the two PC interactions. Their spectral overlap is clearly illustrated in Fig. 1(d) at $k_\perp^2=0$ and the $\Gamma_\parallel$ resonance. This convective gain analysis suggests that cooperative instability growth rates can exceed single-pump instability growth rates by a significant margin and that transverse effects can be important.

While single-pump backward SBS is known to become absolutely unstable when the pump intensity is above $(\alpha F_0^2 L/v)_{\mathrm{SBS}}=v_{\mathrm{ia}}^2 L/4v\omega_0(c_s/c)^2$ [2], the CR pump wave introduces several cooperative absolute instabilities. Intensity thresholds for cooperative absolute instabilities predicted by Eqs. (1)–(6) are plotted in Fig. 2 for two values of the ion damping rate, $\nu_{\mathrm{ia}}/\Omega_{\mathrm{ia}}=0.2$ and 0.05, respectively, and $F_0^2=B_0^2$. In the upper graphs of Figs. 2(a) and 2(b) the threshold intensity is measured in units of the single-pass convective gain for filamentation of the forward pump. The threshold intensity corresponding to $\alpha F_0^2 L/v=1$ is

$$I[\mathrm{W\,cm^{-2}}] \sim \{4.42\times 10^{13} T_{e\mathrm{V}}(1-n_0/n_c)/k_0 L\lambda_\mu^2 (n_0/n_c)\}\,.$$

For $c_s/c=0.001$, $k_0L=1000$, $n_0/n_c=0.25$ and $\lambda_\mu=1.06$ μm, $L=170$ μm and $T_e=940$ eV, so $I=1.1\times 10^{14}$ W cm^{-2}. For these parameters $(\alpha F_0^2 L/v)_{\mathrm{SBS}}=20.0$ and 1.25 for $\nu_{\mathrm{ia}}/\Omega_{\mathrm{ia}}=0.2$ and 0.05, respectively. The real part of the perturbation frequency at these thresholds, $\pm\,\mathrm{Re}(\omega L/v)$, is plotted in the lower graphs of Figs. 2(a) and 2(b). The ion-acoustic frequency of the short-wavelength grating is $\Omega_{\mathrm{ia}}L/v \sim 2k_0 L c_s/c=2$.

In Fig. 2 the lowest nonresonant threshold is plotted as a solid line and has $\omega L/v=0$. The minimal intensity threshold occurs on the nonresonant branch at $\alpha F_0^2 L/v=0.45$ for $k_\perp^2 L/2k_0=3.1$ and is due to cooperative filamentation. In the linear regime light scattered by this cooperative filamentation instability has frequency ω_0 and forms a hollow cone with $\theta_c=(6.2/k_0L)^{1/2}$. This and other signatures of cooperative filamentation have been observed in atomic gas experiments [15]. The dashed curves in Fig. 2(a) and the dotted curves in Fig. 2(b) are the minimal resonant absolute intensity thresholds for $\gamma_{\mathrm{ia}}/\Omega_{\mathrm{ia}}=0.2$ and 0.05, respectively. They are frequency shifted by the acoustic frequency of the $\Gamma_\parallel$ grating. Near $k_\perp=0$ these thresholds have a hybrid character. At large $k_\perp$ they approach the PC threshold. These results show that the cooperative filamentation instability can be important even when cooperative resonant absolute instabilities occur. The cooperative absolute instability intensity thresholds can be much lower than the single-pump thresholds, as stated previously.

The minimum values of the absolute instability thresholds and some of their PC limits are plotted as a function

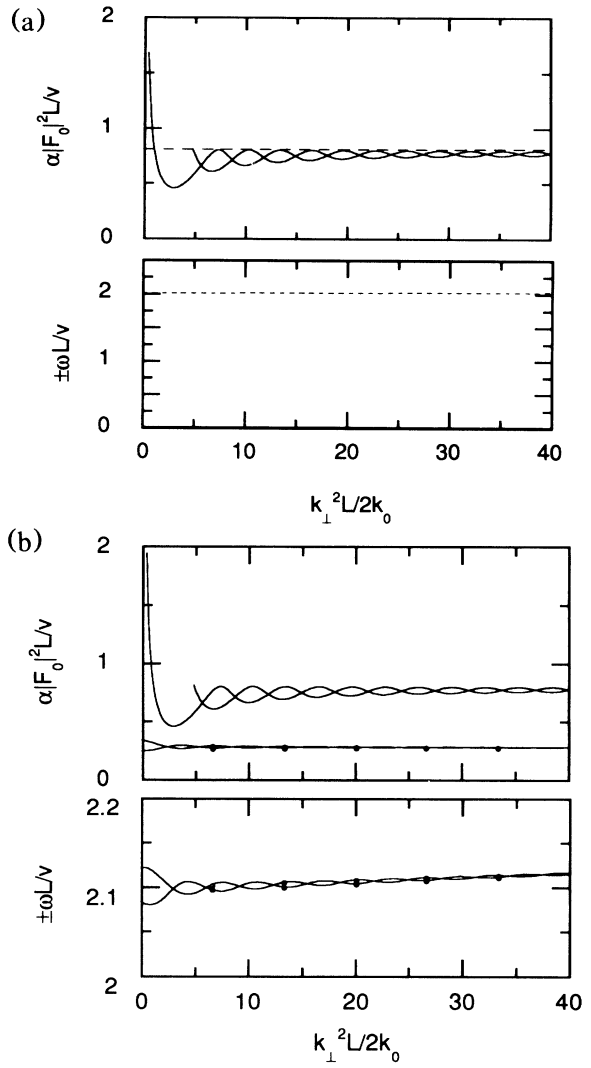

FIG. 2. (a) The resonant (---) and nonresonant (——) absolute thresholds and their frequency shifts for $\gamma_{\mathrm{ia}}/\Omega_{\mathrm{ia}}=0.2$. (b) The resonant (●●●) and nonresonant (——) absolute thresholds and their frequency shifts for $\gamma_{\mathrm{ia}}/\Omega_{\mathrm{ia}}=0.05$.

of $(B_0/F_0)^2$ in Fig. 3 following the labeling convention of Fig. 2. In the limit $(B_0/F_0)^2 \to 1$ the minimal thresholds found in Fig. 2 are recovered. At $(B_0/F_0)^2=1$ the lowest three threshold curves are due to the resonant modes at $\gamma_{\mathrm{ia}}/\Omega_{\mathrm{ia}}=0.05$ where $\alpha F_0^2 L/v=0.24$, 0.28, and 0.33 for $k_\perp^2 L/2k_0=0.0$, 20.0, and 0.0. The nonresonant thresholds are $\alpha F_0^2 L/v=0.45$, 0.72, and 0.79 for $k_\perp^2 L/2k_0=3.1$, 20.0, and 20.0 and the resonant threshold for $\gamma_{\mathrm{ia}}/\Omega_{\mathrm{ia}}=0.20$ is $\alpha F_0^2 L/v=0.80$ at $k_\perp^2 L/2k_0=0.0$. Note that the cooperative TMI threshold given by the $\alpha F_0^2 L/v=0.45$, $k_\perp^2 L/2k_0=3.1$ curve remains degenerate with $\omega=0$ and is below the degenerate phase conjugation threshold over the entire range of r^2 shown. The phase conjugation thresholds for $\alpha F_0^2 L/v=0.72, 0.79$ at $k_\perp^2 L/2k_0=20.0$ can become nondegenerate as shown by the small frequency

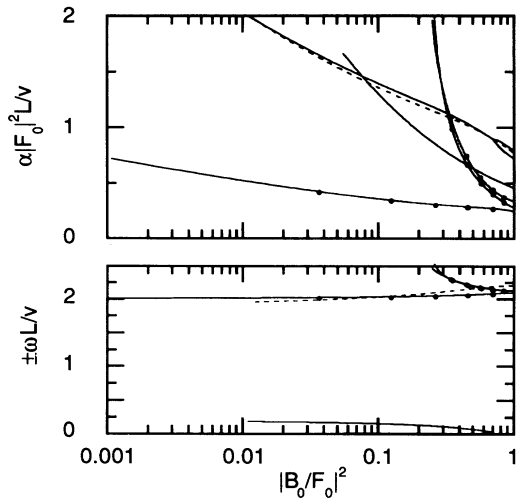

FIG. 3. The minimal absolute thresholds as a function of $(B_0/F_0)^2$ and their frequency shifts.

shift that they acquire as r is decreased. Near $r=1$, this frequency is in agreement with the expected frequency shift of the phase conjugate signal, $(F_0^2-B_0^2)/2$. However, as B_0^2 approaches zero, $\mathrm{Re}(\omega L/v)=0.2$, which is the resonant frequency of $\Gamma_\perp$. Observations consistent with the $k_\perp^2 L/2k_0=0.0$ results are described in [11]. The cooperative absolute instability thresholds are lower than the single-pump or PC thresholds even when the pump intensity ratio is small.

This work can be extended to include three-dimensional geometry [16], plasma inhomogeneity, plasma motion, and distinct pump-wave frequencies. Further work is of particular interest since recent laser-plasma interaction experiments may indicate that a CR pump will enhance the growth of backward SBS or filamentation [17].

The coexistence of single- and multiple-sideband interactions is ubiquitous. When they are simultaneously phase matched the resulting hybrid interaction need not behave as the superposition. A CR light wave introduces cooperative filamentation and cooperative hybrid resonant instabilities which can be attributed to the combined effect of one- and two-sideband instabilities. These cooperative instabilities can have larger convective gains and lower absolute instability thresholds than single-pump instabilities, and their absolute intensity thresholds increase slowly as a function of $(B_0/F_0)^2$. Coupled-wave interactions increase the number of channels by which pump energy can be scattered into sideband modes making them more virulent than single-wave interactions and potentially important in the initiation of the subsequent fully nonlinear evolution.

The authors thank M. V. Goldman for participating in the derivation of the governing equations, as detailed in [16], and both B. B. Afeyan and A. L. Gaeta for many useful conversations. This work was supported by the National Science Foundation under Contract No. 905-7093, by the U.S. Department of Energy Office of Inertial Confinement Fusion under Agreement No. DE-FC03-85DP40200, and by the Laser Fusion Feasibility Project at the Laboratory for Laser Energetics, which is sponsored by the New York State Energy Research and Development Authority and the University of Rochester.

[a]Present address: Arizona Center for Mathematical Sciences, University of Arizona, Tucson, AZ 85721.

[1] J. F. Drake *et al.*, Phys. Fluids **17**, 778 (1974).
[2] B. I. Cohen and C. E. Max, Phys. Fluids **22**, 1115 (1979).
[3] I. M. Begg and R. A. Cairns, J. Phys. D **9**, 2341 (1976).
[4] C. J. Randall, J. J. Thomson, and K. G. Estabrook, Phys. Rev. Lett. **43**, 924 (1979); C. J. Randall, J. R. Albritton, and J. J. Thomson, Phys. Fluids **24**, 1474 (1981).
[5] F. W. Perkins and E. J. Valeo, Phys. Rev. Lett. **32**, 1234 (1974).
[6] G. G. Luther and C. J. McKinstrie, J. Opt. Soc. Am. B **7**, 1125 (1990), and references therein.
[7] S. N. Vlasov and E. V. Sheinina, Radiophys. Quantum Electron. **27**, 15 (1983).
[8] W. J. Firth, A. Fitzgerald, and C. Paré, J. Opt. Soc. Am. B **7**, 1087 (1990), and references therein.
[9] G. G. Luther and C. J. McKinstrie, J. Opt. Soc. Am. B (to be published).
[10] P. Narum *et al.*, J. Opt. Soc. Am. B **5**, 623 (1988).
[11] A. L. Gaeta *et al.*, J. Opt. Soc. Am. B **6**, 1709 (1989).
[12] M. V. Goldman and E. A. Williams, Phys. Fluids B **3**, 751 (1991), and references therein.
[13] A. M. Scott and K. D. Ridley, IEEE J. Quantum Electron. **25**, 438 (1989), and references therein.
[14] W. L. Kruer, *The Physics of Laser Plasma Interactions* (Addison-Wesley, Redwood City, 1988), Chap. 8.
[15] G. Grynberg *et al.*, Opt. Commun. **67**, 363 (1988).
[16] C. J. McKinstrie and M. V. Goldman, J. Opt. Soc. Am. B (to be published).
[17] P. E. Young, H. A. Baldis, and K. G. Estabrook, Phys. Fluids B **3**, 1245 (1991); P. E. Young, Phys. Fluids B **3**, 2331 (1991).